

Received Date : 30-Mar-2016
Revised Date : 21-Jul-2016
Accepted Date : 23-Sep-2016
Article type : Research Article

Discovery of Selective Protein Arginine Methyltransferase 5 (PRMT5) Inhibitors and Biological Evaluations

Sen Ji,^{1,#} Shuang Ma,^{1,#} Wen-Jing Wang,^{1,#} Shen-Zhen Huang,¹ Tian-qi Wang,³ Rong Xiang,³

Yi-Guo Hu,¹ Qiang Chen,¹ Lin-Li Li,^{2,*} and Sheng-Yong Yang^{1,*}

¹*State Key Laboratory of Biotherapy/Collaborative Innovation Center of Biotherapy, West China Hospital, West China Medical School, Sichuan University, Chengdu, Sichuan 610041,*

China

²*West China School of Pharmacy, Sichuan University, Sichuan, China*

³*Department of Clinical Medicine, School of Medicine, Nankai University, Tianjin, 300071, China*

* To whom correspondence should be addressed. Tel.: +86-28-85164063; Fax: +86-28-85164060; E-mail: ysylilinli@sina.com (L-L, Li) oryangsy@scu.edu.cn(S.-Y. Yang)

[#]These authors contributed equally to this work.

This article has been accepted for publication and undergone full peer review but has not been through the copyediting, typesetting, pagination and proofreading process, which may lead to differences between this version and the Version of Record. Please cite this article as doi: 10.1111/cbdd.12881

This article is protected by copyright. All rights reserved.

Abstract

PRMT5 is an important protein arginine methyltransferase that catalyzes the symmetric dimethylation of arginine residues on histones or non-histone substrate proteins. It has been thought as a promising target for many diseases, particularly cancer. Despite the potential applications of PRMT5 inhibitors in cancer treatment, very few of PRMT5i have been publicly reported. In this investigation, virtual screening and structure-activity relationship (SAR) studies were carried out to discovery novel PRMT5i, which finally led to the identification of a number of new PRMT5i. The most active compound, **P5i-6**, exhibited a considerable inhibitory potency against PRMT5 with an IC_{50} value of $0.57\mu M$, and a high selectivity for PRMT5 against other tested PRMTs. It displayed a very good anti-viability activity against two colorectal cancer cell lines, HT-29 and DLD-1, and one hepatic cancer cell line, HepG2, in a sensitivity assay against 36 different cancer cell lines. Western Blot assays indicated that **P5i-6** selectively inhibited the symmetric dimethylations of H4R3 and H3R8 in DLD-1 cells. Overall, **P5i-6** could be used as a chemical probe to investigate new functions of PRMT5 in biology and also served as a good lead compound for the development of new PRMT5-targeting therapeutic agents.

Introduction

Protein arginine methyltransferases (PRMTs) are a family of enzymes that can catalyze the transfer of one or two methyl groups from S-adenosylmethionine (AdoMet) to the guanidino nitrogen atoms of arginine residues on histones and non-histone proteins.¹⁻⁴ PRMTs have been demonstrated to play important roles in a wide variety of cellular functions, including chromatin remodeling, RNA metabolism, signal transduction, embryonic development, and DNA damage repair.⁵⁻⁸ To date, 9 PRMTs have been identified in human,

This article is protected by copyright. All rights reserved.

which can be divided into four categories (type I-IV) according to the products of enzymatic reactions. Type I enzymes catalyze the formation of ω - N^G monomethylarginine (ω -MMA) and asymmetric ω - N^G , N^G -dimethylarginine (ω -aDMA); Type II enzymes catalyze the formation of ω -MMA and symmetric ω - N^G , N^G -dimethylarginine (ω -sDMA); Type III enzymes catalyze the formation of ω -MMA only, and Type IV enzymes catalyze the formation of δ - N^G -MMA.^{3, 4, 9}

Among all the PRMTs, PRMT5, which belongs to the type II PRMTs, has attracted increasing attention in recent years particularly.¹⁰ PRMT5 is 637 amino acids long and maps to human chromosome 14q11.2.^{9, 11} It can symmetrically di-methylate the two-terminal ω -guanidino nitrogen atoms of arginine residues on substrate proteins, including histone H4 at arginine 3 (H4R3me2s)¹²⁻¹⁴, histone H3 at arginine 8 (H3R8me2s)¹⁵, and many other non-histone proteins such as FGF-2¹⁶, NF- κ B¹⁷, HOXA9¹⁸, and p53^{19, 20}. PRMT5 is involved in the transcriptional repression of some tumor suppressor genes, including suppressor of tumorigenicity 7 (ST7)^{15, 21}, nonmetastatic 23 (NM23)¹⁵, retinoblastoma (Rb) family²², and programmed cell death 4 (PDCD4)²³. Besides, PRMT5 has been shown to interact with many other genes, such as p53¹⁹, E2F-1²⁴, IL-2²⁵, cyclin E1²⁶, TRAIL receptor²⁷, MITF²⁸, Schwann Cell Factor 1 (SC1/PRDM4)^{29, 30}, the CDK4 complex³¹, and E-cadherin³², to participate in many cellular processes. Overexpression or dysregulation of PRMT5 was found in a variety of cancers. Recent studies have further demonstrated that this overexpression or dysregulation significantly contributed to the tumorigenesis and development. For example, Nicholas *et al.*²⁸ recently observed a significant upregulation of PRMT5 in human metastatic melanoma cell lines. Powers *et al.*²³ found that PRMT5 was highly expressed in breast cancer, which promoted tumor development by altering tumor suppressor programmed cell death 4 (PDCD4). In a recent study, Bao *et al.*³³ identified a substantial overexpression of PRMT5 in epithelial ovarian cancer, and that this overexpression was associated with poor disease

prognosis. A study by Ibrahim *et al.*³² indicated that a high cytoplasmic expression of PRMT5 was closely related to the high-grade subtypes of primary lung adenocarcinomas and a poor prognosis. All of these indicate that PRMT5 might be a promising therapeutic target in the treatment of cancer.

Due to the potential therapeutic value of PRMT5 inhibitors in cancer therapy, discovery of PRMT5 inhibitors has been one of the research focuses in both industry and academia.³⁴⁻³⁹ However, up to now, very few of PRMT5 inhibitors have been publicly reported.⁴⁰⁻⁴² Thus, in this investigation we tried to discover new potent PRMT5 inhibitors with the aid of computer-aided virtual screening and structure-activity relationship (SAR) analysis.

RESULTS AND DISCUSSION

1. Virtual Screening led to the discovery of a number of hit compounds

Structure-based virtual screening has been demonstrated to be an effective tool for hit or lead discovery, especially in the cases that no ligand or very few of ligands is known.⁴³⁻⁴⁵ Due to the lack of PRMT5 inhibitors, we thus performed a structure-based virtual screening to identify new PRMT5 inhibitors. Currently, there are four X-ray crystal structures of PRMT5 available in RCSB Protein Data Bank (PDB); their PDB entries are 3UA3⁴⁶, 3UA4⁴⁶, 4G56⁴⁷, and 4GQB⁴⁸. 3UA3 and 3UA4 correspond to the structures of *Caenorhabditiselegans* PRMT5, and 4G56 is for the structure of *Xenopuslaevis* PRMT5-MEP50 complexed with S-adenosylhomocysteine (SAH). The remaining 4GQB is for the structure of human PRMT5 in complex with MEP50, an SAH analog, and a peptide substrate derived from histone H4. 4GQB was chosen as the reference structure for the subsequent virtual screening because it is a human PRMT5 structure and has the highest resolution (2.06Å).

To narrow the screening range and also increase the success rate, we constructed a focused library in advance. The construction of the focused library was based on the observation that the active pocket of PRMT5, defined as the binding site of both the cofactor SAM and substrate (see Figure 1A), contains three important residues, namely Glu435, Glu444, and Leu437, which form a perfect hydrogen bonding interaction network with the arginine side chain of substrates (see Figure 1B). To retrieve compounds that can also form a good hydrogen bonding interaction network with the three residues, we first carefully selected fragments that can form multiple hydrogen bonds, including 1, 2-diamines, benzimidamide, semicarbazone, amines, *et al.* Some fragment examples are shown in Figure 1C. Then we searched chemical libraries including SPECS, Chemdiv, Enamine, and our in-house database for compounds that contain any of the selected fragments. These compounds formed a focused library, which includes 1060 small molecules.

Molecular docking-based virtual screening was then carried out to retrieve new PRMT5 inhibitors from the constructed focused library. GOLD version 4.0 was employed for the docking study. From top 100 compounds ranked by the scoring function GoldScore, we carefully selected 56 compounds and subjected to experimental validation. Among the 56 compounds tested, 6 compounds (see Figure 2A) showed an inhibitory rate larger than 50% at a concentration of 50 μ M. The most active compound corresponds to **P5i-6**, which showed an inhibitory rate of 93% at a concentration of 50 μ M, and an IC₅₀ value of 0.57 μ M (see Figure 2B). To further improve its potency, chemical structure modification and SAR studies will be carried out to this compound in the follows.

2. Chemical synthesis

To discuss the SAR of **P5i-6**, we synthesized 25 compounds and purchased 12 compounds from the market. Synthetic routes for the 25 compounds are outlined in Scheme 1-3. Scheme 1 shows the general synthetic routes for compounds **4a-o**. Reaction of 5-bromofuran-2-carbaldehyde (**1**) and triisopropyl borate in n-BuLi easily afforded 5-formylfuran-2-ylboronic acid (**2**), which then reacted with various substituted iodobenzene catalyzed by palladium to give intermediates **3a-o** in good yields. Target compounds **4a-o** were finally obtained through reactions between semicarbazide hydrochloride and corresponding intermediates **3a-o** in ethanol with good yields.

Compounds **6a-c** were synthesized through the similar reaction routes as those for compounds **4a-o**, which are shown in Scheme 2. Treatment of 5-formylfuran-2-ylboronic acid **2** with substituted iodine-containing heterocycles in the presence of sodium carbonate and bis(triphenylphosphine)palladium(II) chloride afforded **5a-c**. The intermediates **5a-c** then reacted with semicarbazide hydrochloride to give target compounds **6a-c** in good yields.

Scheme 3 presents the synthetic routes for compounds **9a-g**. Commercially available (4-chlorophenyl) boronic acid **7** reacted with halogenated aromatic rings, which contain an aldehyde group, in the Suzuki reaction condition to produce intermediates **8a-g**. Then target compounds **9a-g** were obtained through reactions of semicarbazide hydrochloride with corresponding intermediates **8a-g** in the presence of sodium acetate.

3. SAR analysis

The SAR analysis was mainly focused on three regions (see Figure 2C): the two terminal ends, i.e. the 2-methylenediazinecarboxamide moiety (R^1) and the phenyl ring (R^2), and the middle furan ring (R^3).

3.1 Replacement of the 2-methylenediazinecarboxamide moiety (R^1)

To examine the replacement effect of the 2-methylenediazinecarboxamide moiety (R^1), 11 compounds (**1a-k**) with different groups at the R^1 position were purchased from the market. Potencies of these compounds against PRMT5 were first measured at a fixed concentration of 50 μ M. For compounds having an inhibition rate larger than 50% at the concentration of 50 μ M, their IC_{50} values were measured further. Table 1 shows the measured bioactivities of these compounds. Compound **P5i-7**, in which an oxygen atom was simply replaced by a sulfur atom in the 2-methylenediazinecarboxamide moiety, showed a slightly reduced but comparable potency against PRMT5 compared with compound **P5i-6**. However, compounds **P5i-8~P5i-16** with different groups at the R^1 position significantly decreased the bioactivity. These results indicate that the 2-methylenediazinecarboxamide group is a better choice for the R^1 position.

3.2 Variation of the phenyl ring (R^2)

To explore the effect of variation of the phenyl ring (R^2), different groups were introduced at the R^2 position. A total of 18 compounds (**4a-o** and **6a-c**) were synthesized and 2 compounds (**P5i-17** and **P5i-18**) were purchased from the market. Bioactivities of these compounds are displayed in Table 2. From Table 2, we can see that removal of

chlorobenzene (**P5i-17**) or chlorobenzene replaced by -NO₂ (**P5i-18**) led to a complete loss of activity, implying the importance of chlorobenzene at the R² position. Compound **4a** with an unsubstituted phenyl group showed a decreased activity (IC₅₀=12μM). For compounds **4e**, **4g**, **4h**, **4i**, and **4j**, which contain substituents fluoride, nitro, methoxyl, hydroxyl, and amine, respectively, at the para- position of the phenyl ring, their potencies were significantly decreased compared with that of **P5i-6**. For the remaining compounds, which have substituted phenyl, pyridinyl, or pyrimidinyl at the ortho-, meta- and/or para-positions of the phenyl ring, their activities were also substantially reduced compared with that of **P5i-6**.

3.3 Substitution of the middle furan ring (R³)

We finally examined the replacement effect of the middle furan ring (R³). A total of 7 compounds (**9a-g**) with different groups at the R³ position were synthesized. Bioactivities of these compounds are displayed in Table 3. Replacement of the furan ring by thiophene led to a significant decrease in bioactivity. A plausible explanation for this could be that the sulfur atom possesses a larger size than oxygen, which expands the angle between the R¹ arm and the R² arm. In addition, compounds containing a meta-substituted six-membered aromatic ring at R³ (**9b**, **9f**, and **9g**) showed a much higher bioactivity compared with the para-substituted counterparts **9c**, **9d** and **9e**. This again demonstrates the importance of a suitable angle between the R¹ arm and the R² arm.

4. Predicted binding mode of compound **P5i-6** with PRMT5

The above SAR analysis indicates that **P5i-6** is the most active compound against PRMT5 among all the synthesized and purchased compounds. We then analyzed the interaction mode between **P5i-6** and PRMT5. Figure 3 shows the predicted binding mode of **P5i-6** with PRMT5. As expected, the 2-methylenehydrazinecarboxamide moiety of **P5i-6** forms a good hydrogen bonding interaction network with residues Glu435, Leu437, and Glu444 (the hydrogen bonding interaction region). The chlorobenzene moiety perfectly locates in a hydrophobic groove formed by Val326, Phe300, Phe580, Phe577, and Try304 (the hydrophobic region), and good hydrophobic interactions are formed between the chlorobenzene group and residues Phe300, Tyr304, Val326, and Phe580. The middle furan ring, which looks like a bridge that connects the 2-methylenehydrazinecarboxamide and chlorobenzene moieties, is situated at the juncture of the hydrogen bonding interaction region and the hydrophobic region.

5. PRMT Enzyme Selectivity of Compound **P5i-6**

To evaluate the PRMT enzyme selectivity of **P5i-6**, we measured the IC₅₀ values of **P5i-6** against other PRMTs including PRMT1, PRMT3, CARM1 (PRMT4), PRMT6, PRMT7 and PRMT8; PRMT2 and PRMT9 were not included because these enzymes are not available at this moment. The results showed that the IC₅₀ values of **P5i-6** against PRMT1, 3, 4, 6, 7 and 8 were all larger than 100μM (Table 4), suggesting that **P5i-6** has a considerable good selectivity for PRMT5 against other tested PRMTs.

6. *In vitro* sensitivity of various cancer cell lines to P5i-6

The *in vitro* sensitivity of various cancer cell lines to **P5i-6** was examined with 36 cancer cell lines, which cover 17 different cancer types. In this assay, the concentration of **P5i-6** was fixed as 10 μ M and the growth inhibition rate (%) of tumor cells after **P5i-6** treatment for 5 days was measured. The results are summarized in Figure 4. Obviously, several cancer cell lines showed a considerable inhibition rate upon **P5i-6** treatment, and the most sensitive cancer cell lines include two colorectal cancer cell lines, HT-29 and DLD-1, and one hepatic cancer cell line, HepG2. For the other tumor cell lines, **P5i-6** exhibited very weak or no activity, implying that, at least to some extent, the tumor cell growth inhibitory activity of **P5i-6** is not due to its toxic effect.

7. Anti-proliferation effects of P5i-6 against colorectal cancer cell line DLD-1

The tumor cell growth inhibition rate changes over time of **P5i-6** were measured on colorectal cancer cell line DLD-1 for 12 days, which results are summarized in Figure 5A. Obviously the tumor cell proliferation was inhibited in a dose- and time-dependent manner. The inhibitory effect of **P5i-6** against DLD-1 cells was also evident in a colony formation assay, in which a small number of cells were plated and incubated with a series of concentrations of **P5i-6** for 11 days (Figure 5B). We further examined the influence of **P5i-6** treatment on the cell cycle of DLD-1 cells using flow cytometry. The results indicated that a high concentration of **P5i-6** (50 μ M or 100 μ M) led to an increase in the S phase population (see Figure 5C), indicating a S/G2 phase arrest in DLD-1 cells.

8. Inhibition of histone methylation in intact cells

Finally, we examined the inhibitory effects of **P5i-6** to the methylation of substrates of PRMT5 in intact cells by Western Blot. Again, DLD-1 cells were chosen. The results are shown in Figure 5D. **P5i-6** treatment dose-dependently decreased the symmetric dimethylation levels of H4R3 (H4R3me2s) and H3R8 (H3R8me2s), while the asymmetric dimethylation of H4R3 (H4R3me2a) was not affected. These results confirmed, to some extent, the selectivity of **P5i-6** for PRMT5 against other types of PRMTs.^{48, 49} Furthermore, we detected the *ST7* mRNA expression in the time points of day 1 and day 2 after **P5i-6** treatment; *ST7* is a typical target gene of PRMT5.^{15, 21, 39} As shown in Figure 5E, a 1.3-fold increase in *ST7* mRNA expression was observed at day 2, whereas no obvious effect was observed at day 1. These results suggested that **P5i-6** suppressed the catalytic activity of PRMT5.

3. CONCLUSIONS

Structure-based virtual screening and subsequent SAR studies led to the discovery of a number of new PRMT5 inhibitors. The most active compound, **P5i-6**, exhibited a considerable inhibitory potency against PRMT5 with an IC₅₀ value of 0.57μM, and a high selectivity for PRMT5 against other tested PRMTs. 36 different cancer cells were selected to test their sensitivity to **P5i-6**. Several cancer cell lines including two colorectal cancer cell lines, HT-29 and DLD-1, and one hepatic cancer cell line, HepG2, showed a considerable inhibition rate upon **P5i-6** treatment. Flow cytometry was used to examine the influence of **P5i-6** on cell cycles, which results indicated that **P5i-6** treatment arrested the DLD-1 cells in

S/G2 phase. Western Blot assays performed on DLD-1 showed that **P5i-6** could selectively inhibit the symmetric dimethylation of histone H4R3 and H3R8. Collectively, **P5i-6** is a selective PRMT5 inhibitor and could be used as a chemical probe to investigate new functions of PRMT5 in biology. It also could be served as a good lead compound for the development of new PRMT5-targeting therapeutic agents.

4. EXPERIMENTAL SECTION

4.1 Molecular docking. All the molecular docking studies were carried out by GOLD version 4.0 with semi-flexible docking being used. The crystal structure of human PRMT5 (PDB code: 4GQB) was taken as a reference structure for the molecular docking. Before the molecular docking, the receptor protein was prepared by the Discovery Studio (DS) 3.1 (Accelrys Inc., San Diego, CA, USA) software package with standard preparation procedures (protein preparation protocol), which include removing water molecules, adding hydrogen atoms to the protein, and assigning force field (here the CHARMM force field was adopted). The active pocket was defined as the SAH analog and the peptide binding sites. Radius of the site sphere was increased to 16.2Å so that the sphere can cover both the SAM and the substrate binding sites. To explore ring conformations of ligand during docking, the parameter of 'Flip Ring Corners' was chosen, which enables a limited conformational search of cyclic systems by allowing free corners of rings to flip above or below the plane of their neighboring atoms. Other parameters were set to default. GoldScore incorporated into the GOLD program package was employed to predict the binding interaction between small molecules and the receptor protein.

4.2 Compound Sources. Chemical libraries screened include Specs, Enamine, and Chemdiv, as well as our in-house database. Selected compounds were purchased in milligram quantities from chemical vendors. Purity of compounds was $\geq 95\%$, as declared by the chemical vendor.

4.3 Chemistry methods

General procedure for the synthesis of 5-formylfuran-2-ylboronic acid (2) A 500 mL double-neck flask was charged with toluene (100 mL) and cooled to below -60°C , and a solution of n-BuLi (1.6 M in hexanes, 48.6 mL, 77.8 mmol) was added dropwise over 30 min. After the temperature reached to 60°C , a solution of 5-bromofuran-2-carbaldehyde (70.7 mmol) in toluene (30 mL) was added dropwise to keep the temperature below -50°C . A black solid precipitated, and the resultant slurry was stirred for 40 min. THF (30 mL) was added dropwise to keep the internal temperature below -50°C , and the resultant slurry was stirred for 30 min. To the suspension was added triisopropylborate (84.9 mmol) in one portion via syringe. The solution was warmed to 15°C , the reaction was quenched with HCl (aq) (70.0 mL), and the solution was transferred to a pear shape separatory funnel. The aqueous layer was collected, the organic layer was washed with water (30 mL), and the combined aqueous layers were neutralized to pH 7 with NaOH (aq) (12 N) and extracted with EA (300 mL x 3). The combined organics were concentrated in vacuo, and the residue was dissolved in $\text{CH}_2\text{Cl}_2/\text{CH}_3\text{OH}$ (1:1, 140 mL) filtered. The solids were collected by filtration to afford the title compound 2 (6.8 g, 78% yield) as an off-white solid.

General procedure for the synthesis of 5-(4-chlorophenyl)-furan-2-carbaldehyde (3) To a mixture of 5-formylfuran-2-ylboronic acid (2) (1.1 eq) and the substituted iodobenzene (1.0 eq)

in MeCN:H₂O=1:1 (50mL), anhydrous sodiumcarbonate 1.4g (2.0eq) and Pd(PPh₃)₂Cl₂ 470mg (0.1eq) was added. The reaction mixture was stirred in 80°C for 3h, and then cooled to room temperature. The solvent was removed in vacuo. The mixture was treated with water (100 mL) and extracted with EtOAc (3 × 60 mL). The combined organic layers were removed in vacuo. The residue obtained was purified by column chromatography (eluent gradient CH₂Cl₂:MeOH = 80:1) and recrystallized from EtOAc and petroleum ether to get **3** as brown solid.

General procedure for the synthesis of

2-((5-(4-chlorophenyl)furan-2-yl)methylene)hydrazinecarboxamide (4) To a mixture of 5-(4-chlorophenyl)furan-2-carbaldehyde(3) 100mg (1.0eq) in EtOH 10mL, the semicarbazidehydrochloride 54mg (1.0eq) in H₂O 50mL was added dropwise. The reaction mixture was stirred in room temperature for 2h, a white solid precipitated. The solid was filtered in vacuo. The product was washed with water (10 mL) and MeOH (10mL). The residue obtained was purified by column chromatography (eluent gradient CH₂Cl₂:MeOH=20:1) and recrystallized from EtOAc and petroleum ether to get **4** (110mg, 86% yield) as white solid: ¹H NMR (400 MHz, DMSO-*d*₆) δ 10.36 (s, 1H), 7.91-7.73 (m, 3H), 7.49 (d, *J* = 8.5 Hz, 2H), 7.12 (d, *J* = 3.5 Hz, 1H), 6.94 (dd, *J* = 14.9, 3.5 Hz, 1H), 6.46 (s, 2H).

2-((5-phenylfuran-2-yl)methylene)hydrazinecarboxamide (4a) The title compound was obtained in 90% yield, as white solid: ¹H NMR (400 MHz, DMSO-*d*₆) δ 10.34 (s, 1H), 7.80 (d, *J* = 6.0 Hz, 3H), 7.44 (t, *J* = 7.7 Hz, 2H), 7.32 (t, *J* = 7.4 Hz, 1H), 7.07 (d, *J* = 3.5 Hz, 1H), 6.92 (d, *J* = 3.5 Hz, 1H), 6.45 (s, 2H).

2-((5-(2-chlorophenyl)furan-2-yl)methylene)hydrazinecarboxamide (4b) The title compound was obtained in 85% yield, as white solid: ^1H NMR (400 MHz, DMSO- d_6) δ 10.39 (s, 1H), 8.00 (dd, J = 7.9, 1.6 Hz, 1H), 7.81 (s, 1H), 7.64 -7.53 (m, 1H), 7.46 (td, J = 7.7, 1.2 Hz, 1H), 7.36 (td, J = 7.8, 1.6 Hz, 1H), 7.26 (d, J = 3.6 Hz, 1H), 6.98 (d, J = 3.6 Hz, 1H), 6.40 (d, J = 44.6 Hz, 2H).

2-((5-(3-chlorophenyl)furan-2-yl)methylene)hydrazinecarboxamide (4c) The title compound was obtained in 88% yield, as white solid: ^1H NMR (400 MHz, DMSO- d_6) δ 10.35 (s, 1H), 7.86 (t, J = 1.7 Hz, 1H), 7.78 (s, 1H), 7.76 (s, 1H), 7.47 (t, J = 7.9 Hz, 1H), 7.37 (dd, J = 8.0, 1.1 Hz, 1H), 7.21 (d, J = 3.6 Hz, 1H), 6.94 (d, J = 3.6 Hz, 1H), 6.47 (s, 2H).

2-((5-(3-fluorophenyl)furan-2-yl)methylene)hydrazinecarboxamide (4d) The title compound was obtained in 86% yield, as white solid: ^1H NMR (400 MHz, DMSO- d_6) δ 10.36 (s, 1H), 7.77 (s, 1H), 7.65 (d, J = 7.6 Hz, 2H), 7.48 (dd, J = 14.2, 7.7 Hz, 1H), 7.18 (t, J = 2.8 Hz, 1H), 7.01-6.85 (m, 1H), 6.48 (s, 2H).

2-((5-(4-fluorophenyl)furan-2-yl)methylene)hydrazinecarboxamide (4e) The title compound was obtained in 82% yield, as white solid: ^1H NMR (400 MHz, DMSO- d_6) δ 10.31 (s, 1H), 7.85 (dd, J = 8.8, 5.4 Hz, 2H), 7.77 (s, 1H), 7.28 (t, J = 8.9 Hz, 2H), 7.05 (d, J = 3.5 Hz, 1H), 6.91 (d, J = 3.5 Hz, 1H), 6.43 (s, 2H).

2-((5-(2-nitrophenyl)furan-2-yl)methylene)hydrazinecarboxamide (4f) The title compound was obtained in 86% yield, as white solid: ^1H NMR (400 MHz, DMSO- d_6) δ 10.41 (s, 1H), 7.97-7.91 (m, 1H), 7.88 (d, J = 8.0 Hz, 1H), 7.73 (dd, J = 5.5, 2.0 Hz, 2H), 7.62 -7.54 (m, 1H), 7.62 – 7.55 (m, 1H), 7.03 (d, J = 3.6 Hz, 1H), 6.96 (d, J = 3.6 Hz, 1H), 6.41 (s, 2H).

2-((5-(4-nitrophenyl)furan-2-yl)methylene)hydrazinecarboxamide (4g) The title compound

was obtained in 86% yield, as white solid: ^1H NMR (400 MHz, DMSO- d_6) δ 10.28 (s, 1H), 9.76(s,1H), 7.76 (s, 1H), 7.74 (d, J = 1.9 Hz, 1H), 7.73 (d, J = 1.9 Hz, 1H), 7.02 (d, J = 2.7 Hz, 1H), 6.99 (d, J = 2.7 Hz, 1H), 6.91 (d, J = 3.5 Hz, 1H), 6.87 (d, J = 3.5 Hz, 1H), 6.42 (s, 2H).

2-((5-(4-methoxyphenyl)furan-2-yl)methylene)hydrazinecarboxamide (4h) The title compound was obtained in 86% yield, as white solid: ^1H NMR (400 MHz, DMSO- d_6) δ 10.28 (s, 1H), 7.76 (s, 1H), 7.74 (d, J = 1.9 Hz, 1H), 7.73 (d, J = 1.9 Hz, 1H), 7.02 (d, J = 2.7 Hz, 1H), 6.99 (d, J = 2.7 Hz, 1H), 6.91 (d, J = 3.5 Hz, 1H), 6.87 (d, J = 3.5 Hz, 1H), 6.42 (s, 2H), 3.80 (s, 3H).

2-((5-(4-hydroxyphenyl)furan-2-yl)methylene)hydrazinecarboxamide (4i) The title compound was obtained in 86% yield, as white solid: ^1H NMR (400 MHz, DMSO- d_6) δ 10.24 (s, 1H), 9.76 (s, 1H), 7.74 (d, J = 9.2 Hz, 1H), 7.62 (d, J = 8.5 Hz, 2H), 6.87-6.79 (m, 4H), 6.39 (s, 2H).

2-((5-(4-aminophenyl)furan-2-yl)methylene)hydrazinecarboxamide (4j) The title compound was obtained in 86% yield, as white solid: ^1H NMR (400 MHz, DMSO- d_6) δ 10.19 (s, 1H), 7.71 (s, 1H), 7.46 (d, J = 8.4 Hz, 2H), 6.80 (d, J = 3.4 Hz, 1H), 6.67 (d, J = 3.4 Hz, 1H), 6.60 (d, J = 8.5 Hz, 2H), 6.36 (s, 2H), 5.43 (s, 2H).

2-((5-(2,4-dichlorophenyl)furan-2-yl)methylene)hydrazinecarboxamide (4k) The title compound was obtained in 95% yield, as white solid: ^1H NMR (400 MHz, DMSO- d_6) δ 10.37 (s, 1H), 8.07 (t, J = 8.2 Hz, 1H), 7.78 (s, 2H), 7.69 (s, 1H), 7.67 (s, 1H), 7.25 (d, J = 3.6 Hz, 1H), 6.94 (d, J = 3.6 Hz, 1H), 6.48 (s, 2H).

2-((5-(2,3-dichlorophenyl)furan-2-yl)methylene)hydrazinecarboxamide (4l) The title compound was obtained in 90% yield, as white solid: ^1H NMR (400 MHz, DMSO- d_6) δ 10.42

(s, 1H), 7.97 (dd, J = 8.0, 1.4 Hz, 1H), 7.81 (s, 1H), 7.64 (dd, J = 8.0, 1.4 Hz, 1H), 7.47 (t, J = 8.0 Hz, 1H), 7.35 (dd, J = 7.2, 3.8 Hz, 1H), 7.01 (d, J = 3.7 Hz, 1H), 6.47 (s, 2H).

2-((5-(2-amino-4-chlorophenyl)furan-2-yl)methylene)hydrazinecarboxamide (4m) The title compound was obtained in 86% yield, as white solid: ^1H NMR (400 MHz, DMSO- d_6) δ 10.29 (s, 1H), 7.78 (s, 1H), 7.53 (d, J = 8.4 Hz, 1H), 6.96-6.91 (m, 1H), 6.91- 6.85 (m, 2H), 6.64 (dd, J = 8.4, 2.1 Hz, 1H), 6.40 (s, 2H), 5.71 (s, 2H).

2-((5-(3,4-dichlorophenyl)furan-2-yl)methylene)hydrazinecarboxamide (4n) The title compound was obtained in 92% yield, as white solid: ^1H NMR (400 MHz, DMSO- d_6) δ 10.41 (s, 1H), 8.02 (d, J = 8.6 Hz, 1H), 7.80 (s, 1H), 7.75 (d, J = 2.1 Hz, 1H), 7.53 (dd, J = 8.6, 2.1 Hz, 2H), 7.29 (d, J = 3.6 Hz, 1H), 6.99 (d, J = 3.7 Hz, 1H), 6.47 (s, 2H).

2-((5-(5-chloro-2-methoxyphenyl)furan-2-yl)methylene)hydrazinecarboxamide (4o) The title compound was obtained in 86% yield, as white solid: ^1H NMR (400 MHz, DMSO- d_6) δ 10.33 (s, 1H), 7.85 (d, J = 2.6 Hz, 1H), 7.79 (s, 1H), 7.36 (d, J = 2.6 Hz, 1H), 7.34 (d, J = 2.7 Hz, 1H), 7.18 (s, 1H), 7.15 (s, 1H), 7.08 (d, J = 3.5 Hz, 1H), 6.93 (d, J = 3.5 Hz, 1H), 6.47 (s, 2H), 3.94 (s, 3H).

2-((5-(5-chloropyridin-2-yl)furan-2-yl)methylene)hydrazinecarboxamide (6a) The title compound was obtained in 86% yield, as white solid: ^1H NMR (400 MHz, DMSO- d_6) δ 10.42 (s, 1H), 8.63 (d, J = 2.1 Hz, 1H), 8.00 (d, J = 2.5 Hz, 1H), 7.98 (d, J = 2.5 Hz, 1H), 7.91 (s, 1H), 7.88 (s, 1H), 7.23 (d, J = 3.6 Hz, 1H), 6.99 (d, J = 3.6 Hz, 1H), 6.48 (s, 2H).

2-((5-(6-chloropyridin-3-yl)furan-2-yl)methylene)hydrazinecarboxamide (6b) The title compound was obtained in 96% yield, as white solid: ^1H NMR (400 MHz, DMSO- d_6) δ 10.38 (s, 1H), 8.87 (d, J = 2.2 Hz, 1H), 8.22 (dd, J = 8.4, 2.4 Hz, 1H), 7.79 (s, 1H), 7.58 (d, J = 8.4

Hz, 1H), 7.26 (d, J = 3.5 Hz, 1H), 6.95 (d, J = 3.6 Hz, 1H), 6.49 (s, 2H).

2-((5-(2,4-dimethoxypyrimidin-5-yl)furan-2-yl)methylene)hydrazinecarboxamide (6c) The title compound was obtained in 86% yield, as white solid: ^1H NMR (400 MHz, DMSO- d_6) δ 10.31 (s, 1H), 8.89 (s, 1H), 7.76 (s, 1H), 6.89 (s, 2H), 6.49 (s, 2H), 4.07 (s, 3H), 3.96 (s, 3H).

General procedure for the synthesis of 4'-chlorobiphenyl-4-carbaldehyde (8) To a mixture of 4-chlorophenylboronic acid (**7**) (1.1 eq) and the substituted aromatic aldehyde (1.0 eq) in MeCN:H₂O=1:1 (50 mL), anhydrous sodium carbonate 1.26g (2.0 eq) and Pd(PPh₃)₄ 740mg (0.1 eq) was added. The reaction mixture was stirred in 80 °C under N₂ for 3h, then cooled to room temperature. The solvent was removed in vacuo. The mixture was treated with water (100 mL) and extracted with EtOAc (3 \times 60 mL). The combined organic layers were removed in vacuo. The residue obtained was purified by column chromatography (eluent gradient CH₂Cl₂:MeOH=80:1) and recrystallized from EtOAc and petroleum ether to get **8** as brown solid.

2-((5-(4-chlorophenyl)thiophen-2-yl)methylene)hydrazinecarboxamide (9a) The title compound was obtained in 85% yield, as white solid: ^1H NMR (400 MHz, DMSO- d_6) δ 10.36 (s, 1H), 7.91-7.73 (m, 3H), 7.49 (d, J = 8.5 Hz, 2H), 7.12 (d, J = 3.5 Hz, 1H), 6.94 (dd, J = 14.9, 3.5 Hz, 1H), 6.46 (s, 2H).

2-((4'-chloro-[1,1'-biphenyl]-3-yl)methylene)hydrazinecarboxamide (9b) The title compound was obtained in 87% yield, as white solid: ^1H NMR (400 MHz, DMSO- d_6) δ 10.36 (s, 1H), 8.07 (s, 1H), 7.92 (s, 1H), 7.79 (d, J = 8.5 Hz, 2H), 7.71 (d, J = 7.7 Hz, 1H), 7.65 (d, J = 7.8 Hz, 1H), 7.53 (d, J = 8.5 Hz, 2H), 7.48 (t, J = 7.7 Hz, 1H), 6.62 (s, 2H).

2-((4'-chloro-[1,1'-biphenyl]-4-yl)methylene)hydrazinecarboxamide (9c) The title

compound was obtained in 80% yield, as white solid: ^1H NMR (400 MHz, $\text{DMSO}-d_6$) δ 10.33 (s, 1H), 7.87 (s, 1H), 7.82 (d, J = 8.3 Hz, 2H), 7.75 (d, J = 8.5 Hz, 2H), 7.70 (d, J = 8.3 Hz, 2H), 7.53 (d, J = 8.5 Hz, 2H), 6.55 (s, 2H).

2-((5-(4-chlorophenyl)pyridin-2-yl)methylene)hydrazinecarboxamide (9d) The title compound was obtained in 92% yield, as white solid: ^1H NMR (400 MHz, $\text{DMSO}-d_6$) δ 10.56 (s, 1H), 8.87 (d, J = 1.2 Hz, 1H), 8.26 (d, J = 8.4 Hz, 1H), 8.19-8.05 (m, 1H), 7.93 (s, 1H), 7.83 (d, J = 8.4 Hz, 2H), 7.57 (d, J = 8.4 Hz, 2H), 6.69 (s, 2H).

2-((6-(4-chlorophenyl)pyridin-3-yl)methylene)hydrazinecarboxamide (9e) The title compound was obtained in 90% yield, as a white solid: ^1H NMR (400 MHz, $\text{DMSO}-d_6$) δ 10.51 (s, 1H), 8.94 (s, 1H), 8.31 (d, J = 8.1 Hz, 1H), 8.17 (d, J = 8.3 Hz, 2H), 8.02 (d, J = 8.3 Hz, 1H), 7.91 (s, 1H), 7.56 (d, J = 8.3 Hz, 2H), 6.66 (s, 2H).

2-((5-(4-chlorophenyl)pyridin-3-yl)methylene)hydrazinecarboxamide (9f) The title compound was obtained in 95% yield, as white solid: ^1H NMR (400 MHz, $\text{DMSO}-d_6$) δ 10.55 (s, 1H), 8.85 (s, 2H), 8.52 (s, 1H), 7.94 (s, 1H), 7.86 (d, J = 8.4 Hz, 2H), 7.58 (d, J = 8.4 Hz, 2H), 6.75 (s, 2H).

2-((6-(4-chlorophenyl)pyridin-2-yl)methylene)hydrazinecarboxamide (9g) The title compound was obtained in 88% yield, as white solid: ^1H NMR (400 MHz, DMSO) δ 10.62 (s, 1H), 8.15 (dd, J = 13.0, 7.7 Hz, 3H), 7.96 (s, 1H), 7.95 - 7.88 (m, 2H), 7.56 (d, J = 8.5 Hz, 2H), 6.70 (s, 2H).

4.4 *In vitro* Enzymatic Assays

All *in vitro* enzymatic assays were carried out by Shanghai ChemPartner Co. (998 Halei Road, Pudong New Area, Shanghai, 201203, China). To measure the IC_{50} values, 10

concentrations of the target compound were tested. All enzymes were purchased from BPS bioscience (PRMT1, BPS, Cat. No. 51041; PRMT3, BPS, Cat. No. 51043; PRMT4, BPS, Cat. No. 51047; PRMT5, BPS, Cat. No. 51045; PRMT8, BPS, Cat. No. 51052) or Biogenie (PRMT7, Biogenie, Cat. No. M1055). SAM and SAH were purchased from Sigma. Inc (SAM, Sigma, Cat. No. A7007-100MG; SAH, Sigma, Cat. No. A9384-25MG). Compounds were prepared as 10mM stock in DMSO and diluted to final concentration in DMSO when needed. The PRMT enzymes and substrates were incubated with indicated concentrations of compounds in a 384-well plate for 60 min at room temperature. After the reaction, acceptor and donor solutions were added to label the residual substrates of PRMT enzymes. The labeling process was lasting for 60 min at room temperature, followed by the reading endpoint with EnSpire with Alpha mode. The IC₅₀ values were calculated with GraphPad Prism 5.

$$\text{Inhibition \%} = (\text{Max-Signal}) / (\text{Max-Min}) * 100$$

$$Y = \text{Bottom} + (\text{Top-Bottom}) / (1 + 10^{((\text{LogIC}_{50} - X) * \text{Hill Slope}))}$$

Y is inhibition % and X is compound concentration.

SAM was added as a positive control at each experiment.

4.5 Cell lines and culture conditions

All cell lines used were obtained from American Type Culture Collection. These cell lines were cultured in culture medium supplemented with 10% FBS (Caoyuanlyve), 100 U/ml penicillin, and 100 U/ml streptomycin and maintained at 37°C in a CO₂ incubator with 5% CO₂.

4.6 Cell viability assays

In cell viability assays, tumor cells were seeded in 96-well plates with 10 μ M compound or the same amount of DMSO for 5 days. After the drug treatment, 20 μ L of 5 mg/mL MTT (Sigma-Aldrich) reagent was added to each well and incubated for 2–4 hours, and 100% DMSO was used to dissolve the oxidative product. Finally, the light absorption (OD) values, which are proportional to viable cell numbers, were measured with a SpectraMAX M5 microplate spectrophotometer. All experiments were performed in triplicate.

For the analysis of long-term proliferation of DLD-1 cells, cells were plated in 6-well plates at an appropriate density, on days 4 8 and 12, the cells were counted and split back to the original plating density in fresh medium with compound **P5i-6**. Cells were stained with trypan blue to counting the viable cells.

Western blot assays

The Western blot assays were carried out with a similar method as described in literature.⁴⁹ DLD-1 cells were cultured with indicated concentrations of compound **P5i-6**, followed by the lysing with RIPA lysis buffer (Beyotime). All the antibodies were purchased from Abcam.

Quantitative RT-PCR (qRT-PCR)

mRNA was isolated with trizol according to the manufacturer's protocol (Invitrogen). cDNA was generated using the iScriptTM cDNA Synthesis Kit (Bio-Rad), and the RT-PCR reactions were performed using SsoAdvanced SYBR Green Supermix (Bio-Rad) following the manufacturer's instructions. The primers used for qRT-PCR were: *ST7* forward: TGAAAATCAACGACAACCTTG reverse: ATATTAGTGAGGAAGTGCCT *TP73* forward:

GCACCACGTTTGAGCACCTCT reverse: GCAGATTGAACTGGGCCATGA *gapdh*

forward: TGGAAGGACTCATGACCACA reverse: TTCAGCTCAGGGATGACCTT.

Colony formation assay

DLD-1 cells were seeded in 6-well plates incubated with compound **P5i-6**. After treatment for 14 days, cells were stained by crystal violet.

Cell cycle analysis

Flow cytometry was used for cell cycle assays. DLD-1 cells were treated with compound **P5i-6** for 24 h, and then the cells were harvested and washed with PBS. Cell Cycle and Apoptosis Analysis Kit (Beyotime) was used for cell cycle analysis according to the manufacturer's protocol.

ACKNOWLEDGMENT

This work was supported by the 973 Program (2013CB967204), the National Natural Science Foundation of China (81325021, 81473140, 81573349) and the Program for Changjiang Scholars and Innovative Research Team in University (IRT13031).

References

1. Yang Y., Bedford M.T. (2013) Protein arginine methyltransferases and cancer. Nat. Rev. Cancer;13:37-50.
2. Copeland R.A., Solomon M.E., Richon V.M. (2009) Protein methyltransferases as a target class for drug discovery. Nat. Rev. Drug Discov;8:724-732.

3. Bedford M.T., Clarke S.G. (2009) Protein arginine methylation in mammals: who, what, and why. *Mol. Cell*;33:1-13.
4. Wolf S.S. (2009) The protein arginine methyltransferase family: an update about function, new perspectives and the physiological role in humans. *Cell. Mol. Life Sci*; 66:2109-2121.
5. Bedford M.T., Richard S. (2005) Arginine methylation: an emerging regulator of protein function. *Mol. Cell*;18:263-272.
6. Tan C.P., Nakielnny S. (2006) Control of the DNA methylation system component MBD2 by protein arginine methylation. *Mol. Cell. Biol*;26:7224-7235.
7. Pal S., Sif S. (2007) Interplay between chromatin remodelers and protein arginine methyltransferases. *J. Cell. Physiol*;213:306-315.
8. Lee Y.H., Stallcup M.R. (2009) Minireview: protein arginine methylation of nonhistone proteins in transcriptional regulation. *Mol. Endocrinol*;23:425-433.
9. Branscombe T.L., Frankel A., Lee J.H. (2001) PRMT5 (Janus kinase-binding protein 1) catalyzes the formation of symmetric dimethylarginine residues in proteins. *J. Biol. Chem*;276:32971-32976.
10. Mundade R., Wei H., Lu T. (2014) PRMT5, A Pivotal Player in Cancer. *Austin. J. Pharmacol. Ther*;2:1-4.
11. Krause C.D., Yang Z.H., Kim Y.S. (2007) Protein arginine methyltransferases: Evolution and assessment of their pharmacological and therapeutic potential. *Pharmacol. Ther*;113:50-87.
12. Zhao Q., Rank G., Tan Y.T., Li H., Moritz R.L., Simpson R.J., Cunningham, J.M. (2009)

PRMT5-mediated methylation of histone H4R3 recruits DNMT3A, coupling histone and DNA methylation in gene silencing. *Nat. Struct. Mol. Biol.*;16:304-311.

13. Majumder S., Alinari L., Roy S., Miller T., Datta J., Sif S., Jacob S.T. (2010) Methylation of histone H3 and H4 by PRMT5 regulates ribosomal RNA gene transcription. *J. Cell. Biochem.*;109:553-63.

14. Yue M., Li Q., Zhang Y., Zhao Y., Zhang Z., Bao S. (2013) Histone H4R3 methylation catalyzed by SKB1/PRMT5 is required for maintaining shoot apical meristem. *PLoS One*;8:e83258.

15. Pal S., Vishwanath S.N., Erdjument-Bromage H., Tempst P., Sif S. (2004) Human SWI/SNF-associated PRMT5 methylates histone H3 arginine 8 and negatively regulates expression of ST7 and NM23 tumor suppressor genes. *Mol. Cell. Biol.*;24:9630-9645.

16. Bruns A.F., Grothe C., Claus P. (2009) Fibroblast growth factor 2 (FGF-2) is a novel substrate for arginine methylation by PRMT5. *Biol. Chem.*;390:59-65.

17. Wei H., Wang B., Miyagi M., She Y., Gopalan B., Huang D.B., Lu T. (2013) PRMT5 dimethylates R30 of the p65 subunit to activate NF-kappaB. *Proc. Natl. Acad. Sci. U. S. A.*;110:13516-13521.

18. Bandyopadhyay S., Harris D.P., Adams G.N., Lause G.E., McHugh A., Tillmaand E.G., DiCorleto P.E. (2012) HOXA9 methylation by PRMT5 is essential for endothelial cell expression of leukocyte adhesion molecules. *Mol. Cell. Biol.*;32:1202-1213.

19. Scoumanne A., Zhang J., Chen X. (2009) PRMT5 is required for cell-cycle progression and p53 tumor suppressor function. *Nucleic Acids Res.*;37:4965-4976.

20. Berger S.L. (2008) Out of the jaws of death: PRMT5 steers p53. *Nat. Cell*

Biol;10:1389-1390.

21. Pal S., Baiocchi R.A., Byrd J.C., Grever M.R., Jacob S.T., Sif S. (2007) Low levels of miR-92b/96 induce PRMT5 translation and H3R8/H4R3 methylation in mantle cell lymphoma. *EMBO J*; 26:3558-3569.
22. Wang L., Pal S., Sif S. (2008) Protein arginine methyltransferase 5 suppresses the transcription of the RB family of tumor suppressors in leukemia and lymphoma cells. *Mol. Cell. Biol*;28:6262-6277.
23. Powers M.A., Fay M.M., Factor R.E., Welm A.L., Ullman K.S. (2011) Protein Arginine Methyltransferase 5 Accelerates Tumor Growth by Arginine Methylation of the Tumor Suppressor Programmed Cell Death 4. *Cancer Res*;71:5579-5587.
24. Cho E.C., Zheng S., Munro S., Liu G., Carr S.M., Moehlenbrink J., McGouran J. (2012) Arginine methylation controls growth regulation by E2F-1. *EMBO J*;31:1785-1797.
25. Richard S., Morel M., Cleroux P. (2005) Arginine methylation regulates IL-2 gene expression: a role for protein arginine methyltransferase 5 (PRMT5). *Biochem J*;388:379-386.
26. Fabrizio E., El Messaoudi S., Polanowska J., Paul C., Cook J.R., Lee J.H., Sardet C. (2002) Negative regulation of transcription by the type II arginine methyltransferase PRMT5. *Embo Rep*;3:641-645.
27. Tanaka H., Hoshikawa Y., Oh-hara T., Koike S., Naito M., Noda T., Fujita N. (2009) PRMT5, a novel TRAIL receptor-binding protein, inhibits TRAIL-induced apoptosis via nuclear factor- κ B activation. *Mol. Cancer Res*;7:557-569.
28. Nicholas C., Yang J., Peters S.B., Bill M.A., Baiocchi R.A., Yan F., Grever M.R. (2013)

PRMT5 Is Upregulated in Malignant and Metastatic Melanoma and Regulates Expression of MITF and p27Kip1. *PloS one*;8:e74710.

29. Chittka A., Nitarska J., Grazini U., Richardson W.D. (2012) Transcription factor positive regulatory domain 4 (PRDM4) recruits protein arginine methyltransferase 5 (PRMT5) to mediate histone arginine methylation and control neural stem cell proliferation and differentiation. *J. Biol. Chem*;287:42995-3006.

30. Chittka A. (2013) Differential regulation of SC1/PRDM4 and PRMT5 mediated protein arginine methylation by the nerve growth factor and the epidermal growth factor in PC12 cells. *Neurosci. Lett*;550:87-92.

31. Aggarwal P., Vaites L.P., Kim J.K., Mellert H., Gurung B., Nakagawa H., Diehl J.A. (2010) Nuclear cyclin D1/CDK4 kinase regulates CUL4 expression and triggers neoplastic growth via activation of the PRMT5 methyltransferase. *Cancer Cell*;18:329-340.

32. Ibrahim R., Matsubara D., Osman W., Morikawa T., Goto A., Morita S., Fukayama M. (2014) Expression of PRMT5 in lung adenocarcinoma and its significance in epithelial-mesenchymal transition. *Hum. Pathol*;45:1397-1405.

33. Bao X., Zhao S., Liu T., Liu Y., Liu Y., Yang X. (2013) Overexpression of PRMT5 promotes tumor cell growth and is associated with poor disease prognosis in epithelial ovarian cancer. *J. Histochem. Cytochem*;61:206-217.

34. Gu Z.P., Gao S., Zhang F., Wang Z., Ma W., Davis R.E., Wang Z. (2012) Protein arginine methyltransferase 5 is essential for growth of lung cancer cells. *Biochem J*;446:235-241.

35. Yan F., Alinari L., Lustberg M.E., Martin L.K., Cordero-Nieves H.M.,

Banasavadi-Siddegowda Y., Jacob N.K. (2014) Genetic validation of the protein arginine methyltransferase PRMT5 as a candidate therapeutic target in glioblastoma. *Cancer Res*;74:1752-1765.

36. Han X., Li R., Zhang W., Yang X., Wheeler C.G., Friedman G.K., Gillespie G.Y. (2014) Expression of PRMT5 correlates with malignant grade in gliomas and plays a pivotal role in tumor growth in vitro. *J. Neurooncol*;118:61-72.

37. Chung J., Karkhanis V., Tae S., Yan F., Smith P., Ayers L.W., Sif S. (2013) Protein arginine methyltransferase 5 (PRMT5) inhibition induces lymphoma cell death through reactivation of the retinoblastoma tumor suppressor pathway and polycomb repressor complex 2 (PRC2) silencing. *J. Biol. Chem*;288:35534-35547.

38. Gu Z.P., Li Y., Lee P., Liu T., Wan C., Wang Z. (2012) Protein Arginine Methyltransferase 5 Functions in Opposite Ways in the Cytoplasm and Nucleus of Prostate Cancer Cells. *Plos One*;7:e44033.

39. Yan F., Alinari L., Lustberg M.E., Martin L.K., Cordero-Nieves H.M., Banasavadi-Siddegowda Y., Jacob N.K. (2014) Genetic validation of the protein arginine methyltransferase PRMT5 as a candidate therapeutic target in glioblastoma. *Cancer Res*;74:1752-1765.

40. Ang C.M. (2014) 2-(hetero)aryl-benzimidazole and imidazopyridine derivatives as inhibitors of asparagine methyl transferase. WO 2014/128465 A1.

41. Kenneth W. (2014) PRMT5 inhibitors and uses thereof. US 2014/0221345 A1.

42. Kaniskan H.U., Konze K.D., Jin J. (2014) Selective Inhibitors of Protein Methyltransferases. *J. Med. Chem*;58:1596-1629.

43. Yu X.R., Tang Y., Wang W. J., Ji S., Ma S., Zhong L., Li L.L. (2015). Discovery and structure–activity analysis of 4-((5-nitropyrimidin-4-yl) amino) benzimidamide derivatives as novel protein arginine methyltransferase 1 (PRMT1) inhibitors. *Bioorg Med Chem Lett.*;25:5449-5453.
44. Li G.B., Yang L.L., Wang W.J., Li L.L., Yang S.Y. (2013) ID-Score: a new empirical scoring function based on a comprehensive set of descriptors related to protein–Ligand interactions. *J.Chem Inf Model*;53:592–600.
45. Yang J., Wang L.J., Liu J.J., Zhong L., Zheng R.L., Xu Y., Li L.L. (2012) Structural optimization and structure–activity relationships of N2-(4-(4-methylpiperazin-1-yl)phenyl)-N8-phenyl-9H-purine-2,8-diamine derivatives, a new class of reversible kinase inhibitors targeting both EGFR-activating and resistance mutations. *J. Med Chem*;55:10685–10699.
46. Sun L., Wang M., Lv Z., Yang N., Liu Y., Bao S., Xu R.M. (2011) Structural insights into protein arginine symmetric dimethylation by PRMT5. *Proc. Natl. Acad. Sci. U. S. A.*;108:20538-20543.
47. Ho M.C., Wilczek C., Bonanno J.B., Xing L., Seznec J., Matsui T., Brenowitz M. (2013) Structure of the arginine methyltransferase PRMT5-MEP50 reveals a mechanism for substrate specificity. *PLoS One*;8:e57008.
48. Antonysamy S. Bonday Z., Campbell R.M., Doyle B., Druzina Z., Gheyi T., Russell M. (2012) Crystal structure of the human PRMT5: MEP50 complex. *Proc. Natl. Acad. Sci.*;109:17960-17965.
49. Bogdanovich S., Kim Y., Mizutani T., Yasuma R., Tudisco L., Cicatiello V., Tarallo V.

(2016) Human IgG1 antibodies suppress angiogenesis in a target-independent manner. *Signal Transduct Target Ther*;1:15001.

Figure 1. (A) The defined active pocket of PRMT5, which contains both the cofactor SAM binding site and the substrate binding site. (B) The hydrogen bonding interaction network formed between the arginine side chain (left) or an arginine tail-like fragment (right) and residues Glu435, Glu444, and Leu437. (C) Some fragment examples that may form multiple hydrogen bonds.

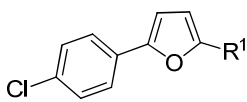
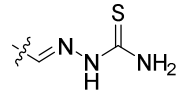
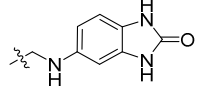
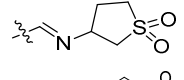
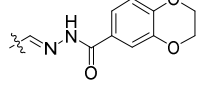
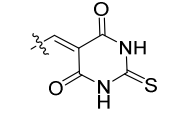
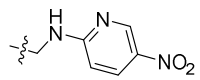
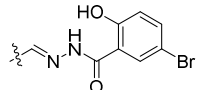
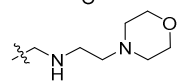
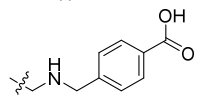
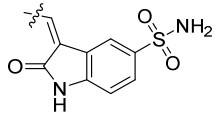
Figure 2. (A) Chemical structures of the 6 compounds (**P5i-1** - **P5i-6**) obtained in a virtual screening that showed an inhibitory rate larger than 50% against PRMT5 at a concentration of 50 μ M. (B) The dose-response curve of **P5i-6** in an enzyme activity assay against PRMT5. (C) Schematic showing regions for SAR analysis.

Figure 3. The predicted binding mode of **P5i-6** in the active pocket of PRMT5

Figure 4. Tumor cell growth inhibition rates of **P5i-6** at a fixed concentration of 10 μ M

Figure 5. (A) The tumor cell growth inhibition rate changes over time of **P5i-6** performed on colorectal cancer cell line DLD-1 for 12 days. Cell vitality was measured using MTT assay at the indicated time points. The growth inhibitory rate is present as percentage of control values (mean \pm SEM, n=3). (B) DLD-1 cells were incubated with indicated concentrations of **P5i-6**. After an 11 days' treatment, the colonies were stained with crystal violet. (C) Cell cycle analysis of DLD-1 cells with the treatment of **P5i-6** for 5 days. Graphs represent the mean of duplicates \pm SEM. (D) The inhibitory effects of **P5i-6** to the methylation of substrates of PRMT5 in intact cells by Western Blot. A series doses of **P5i-6** were added in cultured DLD-1 cells and incubated in 37°C for 3 days before harvest. Specific antibodies for symmetric dimethyl arginine and asymmetric dimethyl of histone4 and symmetric dimethyl arginine of histone3 were used to detect the methylated histone. (E) **P5i-6** induced the transcription of *ST7* in DLD-1 cells. DLD-1 cells were incubated with 10 μ M or 50 μ M **P5i-6** for 1 day or 2 days before harvesting for the RT-PCR assay (mean \pm SEM, n=3). As a control, *gapdh* was also detected.

Table 1. Bioactivities of compounds P5i-7~P5i-16.

			
Compound	R ¹ Group	%Inhibition at 50μM ^a	IC ₅₀ (μM) ^a
P5i-7		83	0.72
P5i-8		N.I.	N.D.
P5i-9		18	N.D.
P5i-10		N.I.	N.D.
P5i-11		58	67
P5i-12		13	N.D.
P5i-13		N.I.	N.D.
P5i-14		20	N.D.
P5i-15		N.I.	N.D.
P5i-16		N.I.	N.D.

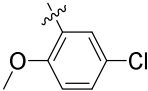
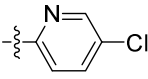
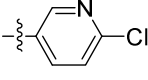
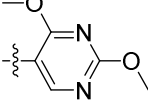
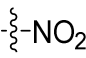
^a IC₅₀ determination experiments were performed in duplicate;

N.I. = no inhibition;

N.D. = not determined

Table 2. Bioactivities of compounds 4a-4o, 6a-6c, P5i-17, and P5i-18..

Compound	R ² Group	%Inhibition at 50μM	IC ₅₀ (μM)
4a		80	12
4b		13	N.D.
4c		23.	N.D.
4d		66	14
4e		82	12
4f		44	N.D.
4g		60	18
4h		90	2.1
4i		22	N.D.
4j		50	40
4k		38	N.D.
4l		28	N.D.
4m		70	13
4n		16	N.D.

4o		17	N.D.
6a		22	N.D.
6b		15	N.D.
6c		6	N.D.
P5i-17	N.S.	0	N.D.
P5i-18		0	N.D.

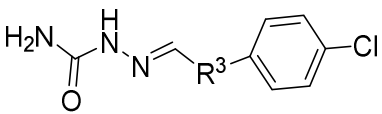
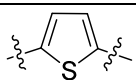
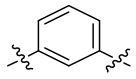
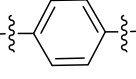
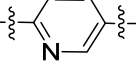
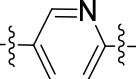
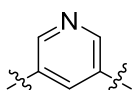
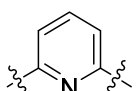
^a IC50 determination experiments were performed in duplicate

N.I. = no inhibition

N.D. = not determined

N.S. = no substitution

Table 3. Bioactivities of compounds 9a-g.

			
Compound	R ³ Group	%Inhibition at 50μM	IC ₅₀ (μM)
9a		33	N.D.
9b		83	3.8
9c		8	N.D.
9d		15	N.D.
9e		4	N.D.
9f		73	6.9
9g		91	3.5

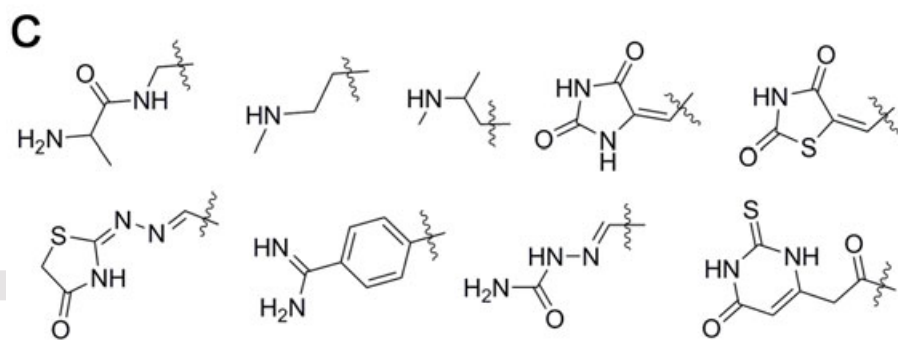
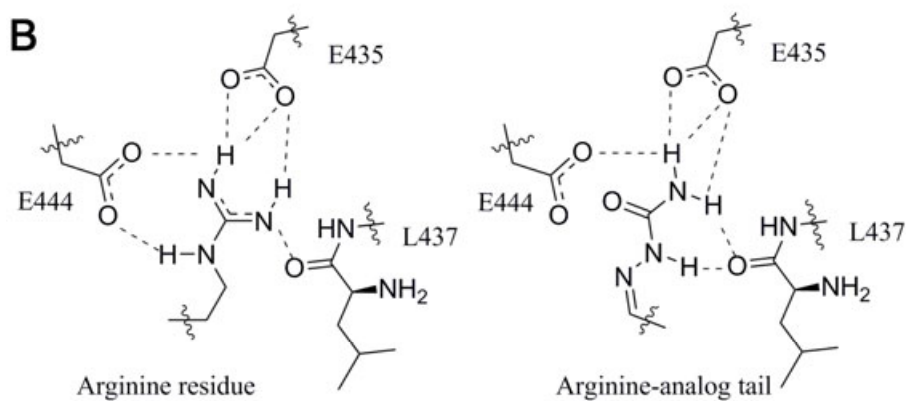
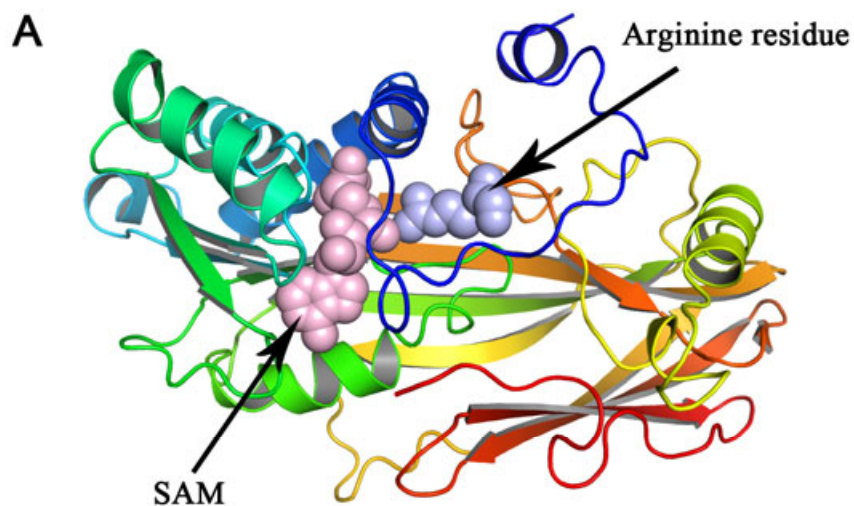
^a IC₅₀ determination experiments were performed in duplicate

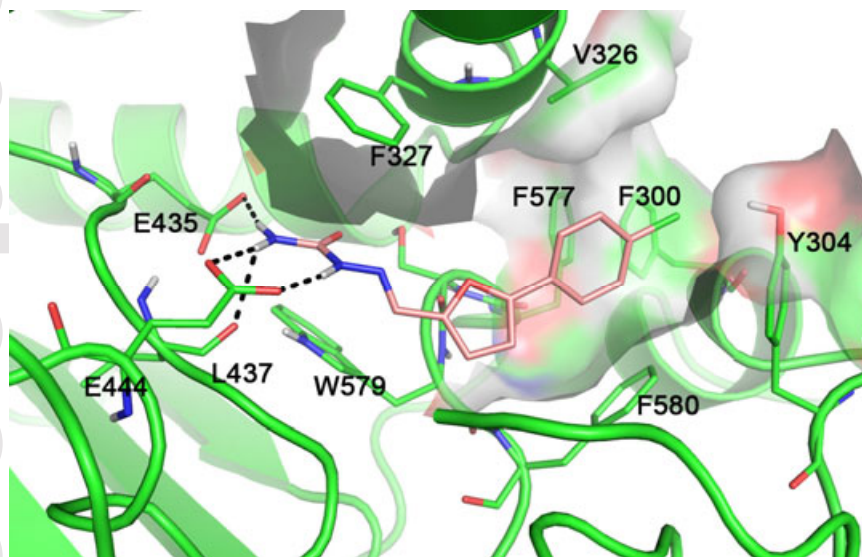
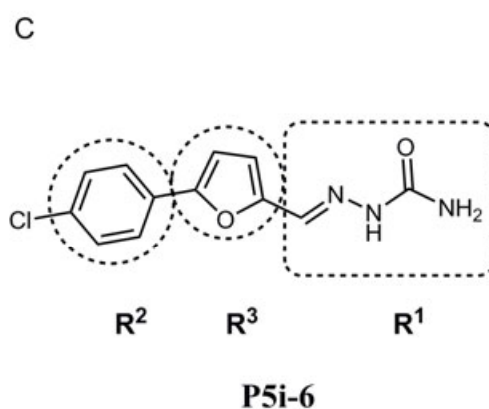
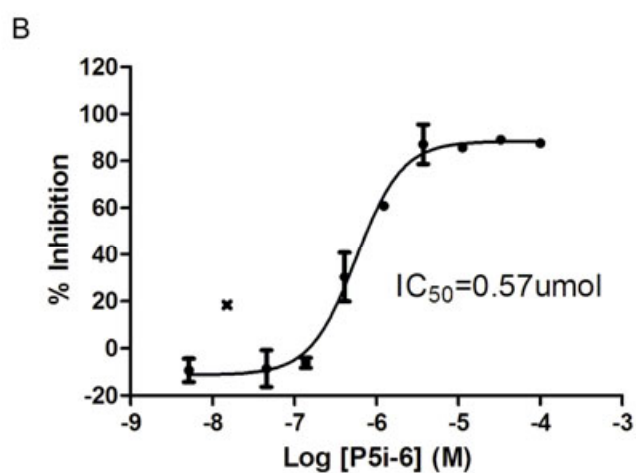
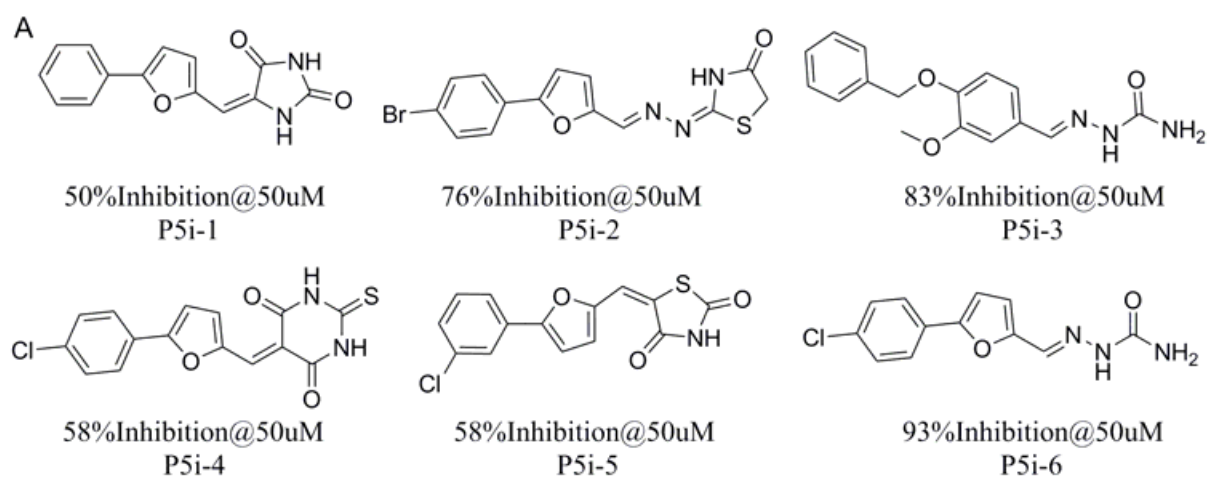
N.I. = no inhibition

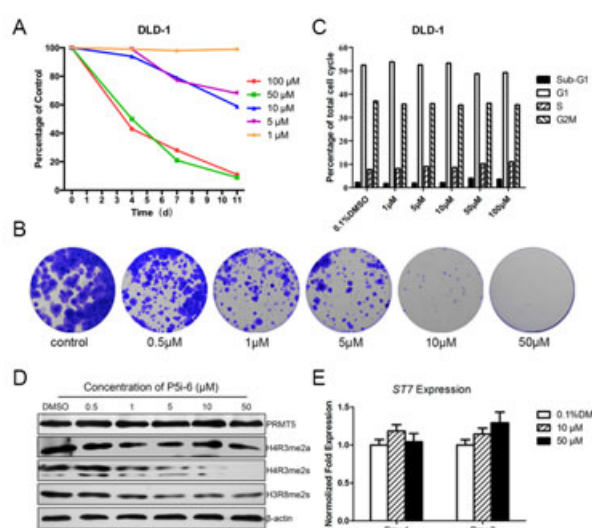
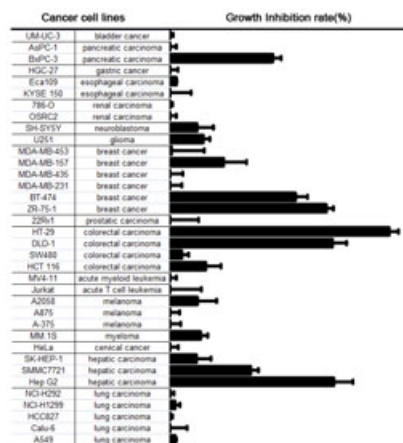
N.D. = not determined

Table 4.IC₅₀ values of Compound **P5i-6** against different PRMTs.

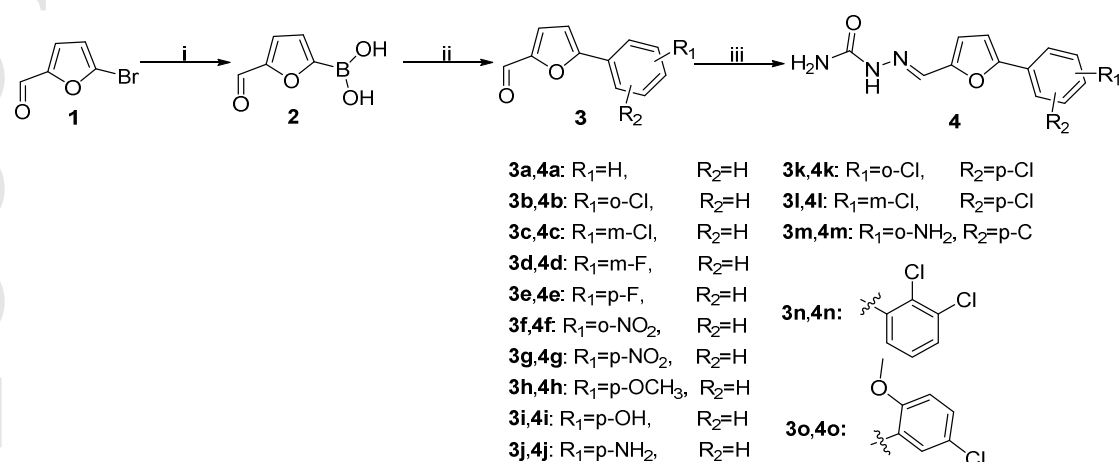
Compounds	IC ₅₀ (μM)					
	PRMT1	PRMT3	CARM1	PRMT6	PRMT7	PRMT8
Pi5-6	>100	>100	>100	>100	>100	>100







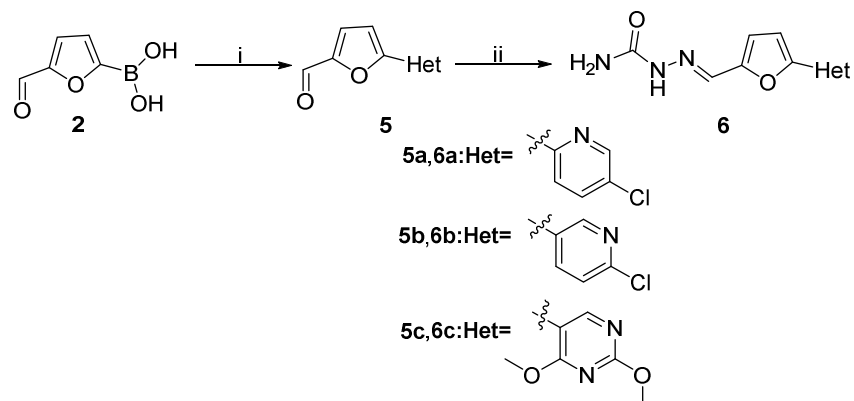
Scheme 1^a. The general synthetic routes for compounds **4a-o**.



^aReagents and conditions: (i) n-BuLi, B(OiPr)₃, HCl(aq), NaOH(aq); (ii) substituted

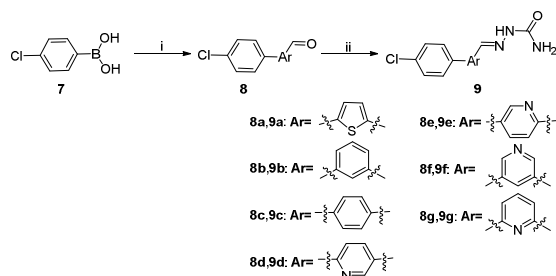
iodobenzene, Na_2CO_3 , $\text{Pd}(\text{PPh}_3)_2\text{Cl}_2$, $\text{MeCN}:\text{H}_2\text{O}=1:1$, 80°C ; (iii) semicarbazide hydrochloride, NaOAc , EtOH , H_2O

Scheme 2^a. The synthetic route for **6a-c**



^aReagents and conditions: (i) iodine-containing heterocycles, Na_2CO_3 , $\text{Pd}(\text{PPh}_3)_2\text{Cl}_2$, $\text{MeCN}:\text{H}_2\text{O}=1:1$, 80°C ; (ii) semicarbazide hydrochloride, NaOAc , EtOH , H_2O

Scheme 3^a. The synthetic routes for compounds **9a-g**.



^aReagents and conditions: (i) $\text{Pd}(\text{PPh}_3)_4$, the substituted aldehyde, Na_2CO_3 , $\text{DME}:\text{H}_2\text{O} = 2:1$; (ii) semicarbazide hydrochloride, NaOAc , EtOH , H_2O